Appl. Magn. Reson. (2008) 34, 289–299
DOI 10.1007/s00723-008-0127-3
Printed in The Netherlands

Applied
Magnetic Resonance

High-Field DNP Spectrometer for Liquids

V. P. Denysenkov[1], **M. J. Prandolini**[1], **A. Krahn**[2,3], **M. Gafurov**[1], **B. Endeward**[1], and **T. F. Prisner**[1]

[1] Institute for Physical and Theoretical Chemistry, Center for Biomolecular Magnetic Resonance, J. W. Goethe University, Frankfurt am Main, Germany
[2] Bruker Elektronik GmbH, Rheinstetten, Germany
[3] Laboratoire de Chimié, Unité Mixte de Recherche, Centre National de la Recherche Scientifique, Ecole Normale Supérieure, Lyon, France

Received 22 October 2007; revised 20 February 2008

Abstract. The construction of a prototype 400 MHz/260 GHz (9.2 T) liquid-state dynamic nuclear polarization (DNP) spectrometer is described. For this purpose a 400 MHz Bruker Avance nuclear magnetic resonance spectrometer was extended with a 260 GHz microwave setup including microwave sources (45 mW continuous-wave and 200 mW pulsed output power), a metal-dielectric waveguide transmission system for decoupling of microwave excitation and reflection, which can also be used for electron paramagnetic resonance (EPR) detection, and special double-resonance structures which have been developed to avoid microwave heating of aqueous samples during DNP experiments. Microwave performance and first EPR and DNP applications on nitroxide radicals in water at room temperature are presented.

1 Introduction

Sensitivity of high-resolution nuclear magnetic resonance (NMR) spectrometers is a limiting factor in the study of large biomolecules in vitro and in vivo. A general approach to overcome this limitation is the employment of higher magnetic fields, which is rather expensive and technically not feasible above a certain field. Application of cryoprobes that can improve NMR sensitivity by another factor of three is also at the technical limit [1]. A very promising alternative is the dynamic nuclear polarization (DNP) method that can increase the sensitivity of NMR measurements up to a factor of 660 for protons. DNP is a method to transfer the much higher electron spin polarization to nuclei by microwave (MW) irradiation of electron paramagnetic resonance (EPR) transitions. Successful DNP experiments showing impressive signal enhancements have been performed at low temperatures in the solid state [2, 3] or at low magnetic fields in liquids [4, 5]. Both methods have drawbacks because the sample has to be transferred fast to the high magnetic field and/or melted.

Here we describe a different approach, in which an aqueous sample is irradiated by microwaves (260 GHz) and NMR detected (400 MHz) at the same magnetic field (9.2 T) in the liquid state. This procedure could significantly improve the quality of liquid-state NMR and extend the structure determination to larger biological macromolecules.

The demanding objective is to develop a spectrometer with NMR, DNP and EPR capabilities facilitating the optimization of the DNP effect. The DNP enhancement is proportional to the square of the irradiating MW magnetic field below saturation of the EPR transitions. Hence, it is important to increase this MW field strength as much as possible. This may be achieved by placing the sample into a resonant structure instead of using a nonresonant waveguide. In the past years similar attempts have already been discussed for solid-state NMR and corresponding hardware has been designed. For example, a spectrometer described by Singel et al. [6] is equipped with a double-resonance structure consisting of a Fabry–Perot resonator for EPR and MW pumping, and a radio frequency (RF) coil located between spherical mirrors of the resonator. Novel DNP-NMR probes on a horn reflector and an oversized MW cavity presented by Wind and coworkers [7] enabled DNP experiments at room temperatures in nonlossy samples. Recently, a low-temperature probe for DNP-NMR was reported by Cho et al. [8] exploiting a double resonance structure on the basis of a double-horn cavity configuration. In all above cases the developed structures can be used for solids and nonlossy liquids.

We have built a 9.2 T DNP spectrometer to investigate the potential of an NMR sensitivity improvement on biomolecules in liquid solution at room temperature. For this purpose, a 400 MHz Bruker Avance NMR spectrometer was extended with a homebuilt 260 GHz MW bridge. It contains two MW sources (45 mW continuous-wave [CW] and 200 mW pulsed power), a metal-dielectric waveguide transmission system, and some double-resonance structures for aqueous samples. The spectrometer is designed for in situ NMR, EPR, and DNP experiments where MW and RF pulses can be applied at the same time.

In this paper, we describe the construction of the spectrometer and show first results to demonstrate the potential of DNP in combination with high-resolution NMR. Usually, a sample for DNP experiments contains an aqueous solution of the biomolecules under study and an added paramagnetic dopant that interacts either directly or indirectly with the nuclei of the biomolecule. EPR experiments on such aqueous samples suffer from extremely high insertion losses in water as determined by the dielectric permittivity ε'' and ε' at MW frequencies. Even more difficulties are expected for DNP experiments due to the higher MW power in comparison with EPR, causing extensive heating of the sample. In the submillimeter wave range the permittivity in water is lowered reaching $\varepsilon'' = 5.8$ and $\varepsilon' = 5.6$ at 260 GHz [9], but losses are still high enough to cause an unacceptable MW heating of biological samples.

Additionally, DNP enhancement studies on radical solutions in the liquid state at the magnetic fields indicate that the enhancement should decrease at least 5 times while the field increases from 0.1 to 5 T [10]. However, up to now it was neither investigated for coupled three-spin systems (*S–I–I* or *S–S–I* with an

electron spin S and a nuclear spin I) nor for more advanced pulsed MW and RF excitation schemes. Here, we present our first experimental results on a nitroxide radical in water at room temperature.

2 Description of the Spectrometer

2.1 System Configuration and Equipment

The DNP spectrometer setup (Fig. 1) is based on a high-resolution NMR spectrometer. The spectrometer consists of a room-temperature wide-bore 9.4 T cryomagnet (Bruker) which can be swept by ± 40 mT and a 400 MHz NMR console (Bruker Avance). An MW bridge operating in the range from 255 to 263 GHz is used for pumping the electron spin transitions and EPR detection. The probehead comprises a double-resonance structure which is located in the center of the room-temperature bore of the cryomagnet and is connected to the MW bridge and NMR console. An EPR spectrum can be recorded by a Stanford Research SR510 lock-in amplifier in conjunction with a computer-controlled Wavetek Model 23-function generator.

2.2 Microwave Bridge

Our DNP approach allows simultaneous irradiation of an aqueous sample by MW 260 GHz and 400 MHz RF. The 400 MHz NMR experiment is operated by a commercially available Bruker Avance spectrometer, while the sample irradiation can be performed with the 260 GHz MW bridge, which is designed especially for this DNP spectrometer. The bridge allows switching between two MW sources:

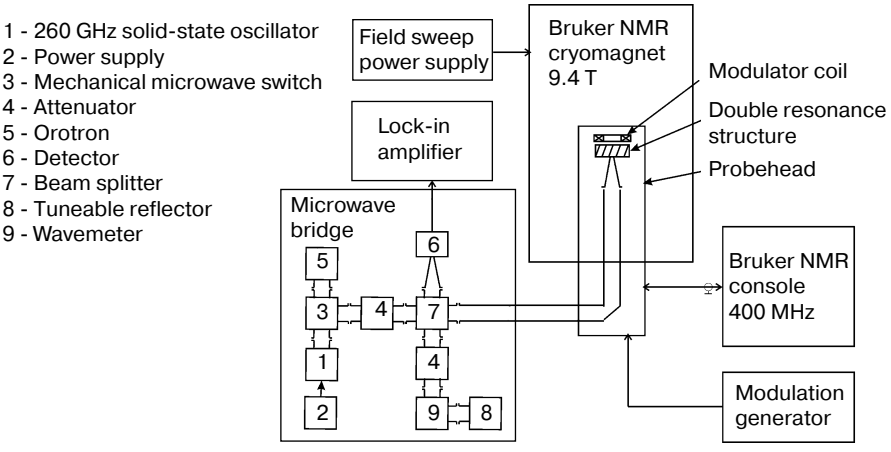

Fig. 1. Schematic diagram of the DNP spectrometer.

a 45 mW VDI-S019b solid-state MW source (Virginia Diodes Inc., Charlottesville, VA, USA), powered by a homebuilt power supply, and an orotron with 200 mW pulse peak output power (GYCOM, Nizhnij Novgorod, Russia). The waveguide transmission system of the bridge consists of oversized waveguides, attenuators, a beam splitter, a wavemeter and a reflector which were designed and built by the Institute of Radiophysics and Electronics in Kharkiv, Ukraine. The MW-detector is a VDI-WR3ZBD-S027C zero-bias Schottky diode (Virginia Diodes Inc.).

The solid-state source (position 1 in Fig. 1) consists of a temperature-stabilized yttrium iron garnet (YIG) oscillator operating in a CW mode. It can be tuned in a frequency range of 15.3–16.6 GHz and has a low-phase noise due to the high Q-factor of the applied YIG resonator. After a chain of multiplication–amplification stages an MW signal of 40–50 mW in the 245–265 GHz range is available. Usually, we use a narrow frequency range of 255–260 GHz limited by the control voltage of the power supply in the sweep mode to check the resonator performance before experiments. The spectral purity of the signal is mostly defined by the YIG oscillator with a phase noise of about -105 dB/Hz at 10 kHz offset, multiplied by a factor of 16, according to the frequency multiplication chain. Therefore, the source meets the requirements necessary to perform DNP and EPR experiments. The long-term frequency drift of the MW source defined by the relative control voltage instability is about $2 \cdot 10^{-5}$ per hour, which is enough to measure nitroxide radicals for half an hour without evident distortions of the EPR line. The frequency instability of the source is a limiting factor only for paramagnetic molecules with a very narrow EPR line (less than 0.1 mT), which is unusual at such high magnetic fields. The orotron (position 5 in Fig. 1) is a MW vacuum tube device operating in a pulse mode with 10% duty cycle and 200 mW MW peak power in the frequency range from 120 up to 260 GHz. The long-term frequency stability of the orotron is defined by a relative instability of the power supply which is about $5 \cdot 10^{-6}$ per hour.

The MW network of the spectrometer was designed to minimize MW losses and to allow high-sensitive EPR detection at the same time. The 260 GHz frequency corresponds to a wavelength in the millimeter and submillimeter range. In this frequency range both a quasioptical system of appropriate dimensions and a system based on the oversize waveguide components can be applied. Our current version of the MW bridge is based on a so-called metal-dielectric waveguide which is a square cross-section metal tube with lateral dimensions essentially exceeding the wavelength and an inner surface coated with a dielectric layer. The bridge can operate in different modes to cover all necessary tasks: cavity tuning mode, EPR detection mode and DNP mode.

Decoupling of the EPR detection from the MW excitation is accomplished by configuring the MW bridge as a Michelson interferometer. This configuration has high sensitivity in the EPR detection mode (Fig. 2). Such interferometers are commonly used in EPR spectrometers with reflected signal detection [11]. Our interferometer has a signal arm (from position 7 to the double-resonance structure in Fig. 1) and a reference arm (from position 7 to position 8 in Fig. 1) of the same length. The best EPR sensitivity is achieved when the beam splitter couples half of the incident power into the adjacent reference arm (the 3 dB

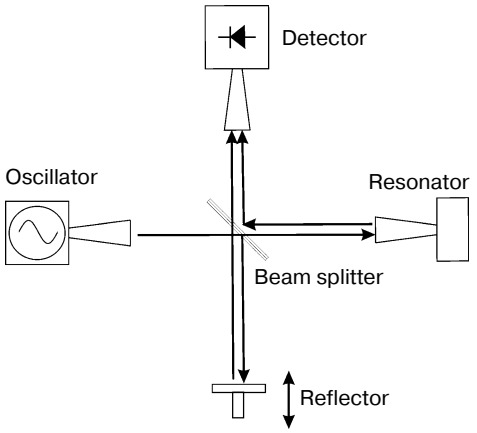

Fig. 2. Schematic representation of the reflection mode MW configuration for the DNP spectrometer.

option). The interferometer has 0.7 dB losses in each arm, and its isolation reaches −34 dB when both arms are in phase (bridge balance). The 3 dB splitting is optional for EPR, but not optimal for operating in DNP mode when a maximum MW power has to be applied to the sample. For this purpose, the beam splitter can be exchanged for one with a larger splitting ratio. In our case, the optional splitting ratio is about 24 dB, meaning 99.5% of the power is transmitted to the signal channel, while 0.5% of the power goes to the reference arm preventing the saturation of the MW detector (position 6 in Fig. 1). The bridge has less than 2 dB of total propagation losses from the source to the double-resonance structure, therefore at least 22 mW of incident MW power reaches the sample for the critical coupled resonance structure.

2.3 DNP Probehead

The DNP probe contains the double-resonance structure, RF tuning setup, and the MW waveguide. The performance of the spectrometer strongly depends on the efficiency of the probe, which is mainly defined by the resonance structure. Our first approach is a double-resonance structure similar to one described by Weis et al. [12] rescaled to the 260 GHz operation (Fig. 3). The resonance structure is a cylindrical TE_{011} MW cavity, where the slotted cylinder of the cavity serves as the RF coil. A copper tape is used forming a helical six-turn coil with an inner diameter of 1.48 mm. The leads of the coil are connected to the RF circuit tuned to a 400 MHz NMR frequency. This arrangement permits RF penetration as previously explored by Gruber et al. [13] at lower frequencies. The MW cavity part inside of the helix is equipped with two plungers made of polychlorotrifluoroethylene with flat caps coated with a thin silver film. For frequency tuning, one of the plungers can be moved outside the probe via gears and a driving rod. The second plunger has no remote control and is tuned manually before the probe

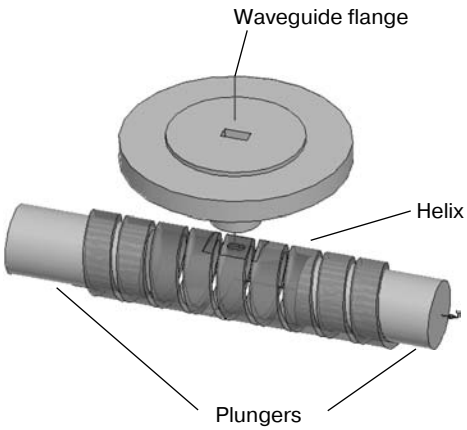

Fig. 3. Schematic drawing of the MW and RF double resonance structure used for our measurements.

installation into the cryomagnet. MW coupling is achieved through an elliptical centered iris via a WR-4 waveguide that touches the helix in the middle, grounding the coil at this position with respect to RF (Fig. 4). The angular electric field distribution of TE_{01n} modes is maintained since the gaps between turns are almost parallel to the surface currents. Moreover, the gaps serve as a filter for other unwanted modes, so that the cavity shows a clear MW spectrum of only TE_{01n} modes. The resonance structure was simulated for frequency response, magnetic field distribution, and calculations of Q-factor as well as B_1 value using the Ansoft high-frequency structure simulator (HFSS) software (Ansoft Corp., Pittsburgh, PA, USA).

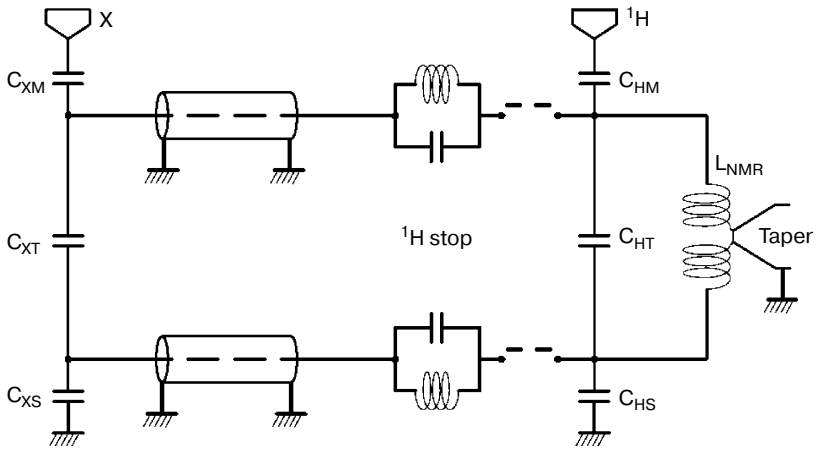

Fig. 4. RF circuit design.

The helix coil is tuned to a 392 MHz proton frequency by a parallel capacitance C_{HT} and matched to the line impedance of the 50 Ω feeding line by the capacitance C_{HM}. To symmetrically drive the coil, e.g., to compensate imbalances due to the RF coupling, we use an extra capacitance C_{HS} connected to ground. In case of a perfectly symmetrically driven solenoid, the current is maximum in the central turn corresponding to virtual ground [14]. Thus, the RF field distortion resulting from the electrical contact between the grounded waveguide and the central turn of the solenoid is minimized. For further experiments, this circuit may be extended with a symmetric circuit for the X channel, electrically isolated by two proton stop circuits.

The probehead is further equipped with a modulation coil which is placed above the helix for EPR detection and operates in the range of modulation frequencies between 1 and 100 kHz with an amplitude up to 0.5 mT. It is important to select the proper pumping frequency for DNP experiments. In a CW EPR experiment, the magnetic field and the frequency can be swept. Magnetic field sweep is preferred because it covers up to ±40 mT and is free of phase distortions. Frequency sweep is limited by the resonator band width, which is about 500 MHz. Additionally, the EPR spectrum can be distorted by changing the admixture of absorption and dispersion during the frequency sweep and also via standing waves in the waveguide. In future, we plan to equip the probe with a temperature control to perform measurements at various temperatures. The spectrometer specifications are shown in Table 1.

3 Sample Conditions and Properties

We used a solution of 6.4 mM 2,2,6,6-tetramethylpiperidine-N-oxyl-4-ol (TEMPOL) from Sigma-Aldrich in distilled water [5, 15] to test the DNP performance of the spectrometer at room temperature. Nitroxide radicals are of interest for biological applications because in vivo studies have not yet revealed any serious toxicity problems when nitroxides are injected intravenously [16–19] and they can be covalently attached to biomolecules [20–23], especially suiting them for targeting studies. Nitroxides exhibit three EPR lines due to the hyperfine splitting arising from the interaction between the electron spin and a nitro-

Table 1. General specifications of the DNP spectrometer.

Magnetic field sweep range (T)	9.16–9.24
MW frequency sweep range (GHz)	255–260
MW power, minimum (mW)	
in CW mode	45
in pulse mode	200
MW transmission losses, maximum (dB)	1.8
MW cavity Q-factor without a sample, maximum	650
MW B_1 conversion factor, maximum (mT/W$^{0.5}$)	1.0
RF B_2 conversion factor, maximum (mT/W$^{0.5}$)	0.17

gen nucleus of spin $I = 1$. The hyperfine structure obviously affects the saturation properties of the EPR spectrum.

For our first test experiment the sample was introduced into quartz capillaries with an inner diameter of 0.05 or 0.1 mm (from Polymicro Technologies). The actual sample volume can be defined from the distance between the plungers (1.6 mm in the case of TE_{011} mode) which results in a total sample volume of 12 nl (in 0.1 mm capillary) effected by MW irradiation during the DNP experiment.

4 Results and Discussion

The MW performance of the probe was evaluated by measuring the Q-factor and MW coupling of the helix containing an empty and water-filled capillary with an inner diameter of 0.1 mm (Fig. 5). We calculated the MW conversion factor C_{MW} of the structure with the sample using the Ansoft HFSS software and measured the MW Q-values, which are presented in Table 2.

The RF performance of the helix was evaluated by measuring the ^{1}H NMR 90°-pulse length and the signal-to-noise ratio of the NMR signal. The 90°-pulse length is about 20 μs at the applied RF power of 3 W which results in an RF conversion factor of about 0.17 mT/W$^{0.5}$. At this stage we did not attempt to homogenize the external magnetic field over the sample to minimize the line shape distortions and broadening.

The EPR performance of the spectrometer was tested with a field scan across the EPR spectrum of the aqueous TEMPOL solution as described in Sect. 3 (Fig. 6). The power dependence of the signal amplitude was measured in order to estimate the saturation parameter, which is an important parameter for the

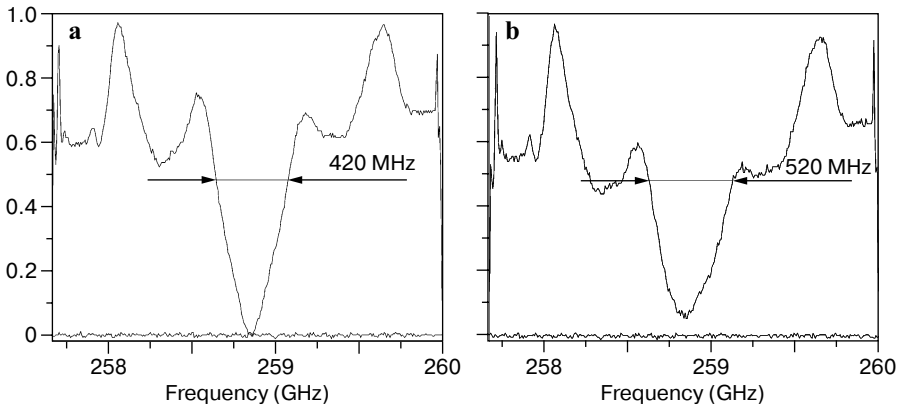

Fig. 5. MW frequency response of the double-resonance structure. The reflected MW power is shown as a function of the MW frequency. The bandwidth of the mode is indicated by arrows. Additionally, periodic standing waves from the waveguide can be seen on both sides of the resonant curve of the cavity. **a** Resonator mode with an empty capillary (inner diameter, 0.1 mm; outer diameter, 0.16 mm). **b** Resonator mode with the same capillary filled with water.

Table 2. Calculated for B_{1max} and measured (Q-factor) MW parameters of the helix cavity.

Cavity length (mm)	Operation mode	Q-factor (empty capillary)	Q-factor (capillary with water)	C_{MW} (mT/W$^{0.5}$)
1.6	TE_{011}	600	410	1.0
3.2	TE_{012}	650	500	0.55

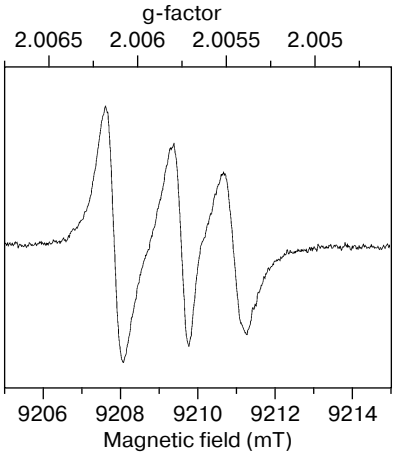

Fig. 6. CW EPR spectrum of a 6.4 mM aqueous TEMPOL solution with 0.25 mW MW power at 258.54 GHz using the helix resonance structure. Single scan at 0.02 mT/s with 1 s time constant. The magnetic field was calibrated by measuring ^{1}H NMR signal of water molecules; the microwave frequency of the driver oscillator was measured by the HP5342A frequency counter. This allows to determine accurate *g*-factor values. The line shape can be explained by the molecular tumbling of the nitroxide radical visible at the high EPR frequency of 260 GHz [23].

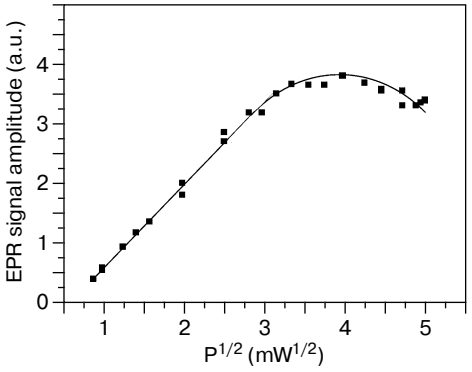

Fig. 7. EPR signal amplitude (first hyperfine line) dependence on applied MW power for 6.4 mM TEMPOL in water in 0.1 mm (inner diameter) capillary measured at room temperature at 260 GHz. The saturation curve is a result of fits based on a least-squares method with the parameter $T_1T_2 = 3.5 \cdot 10^{-15}$ s^2.

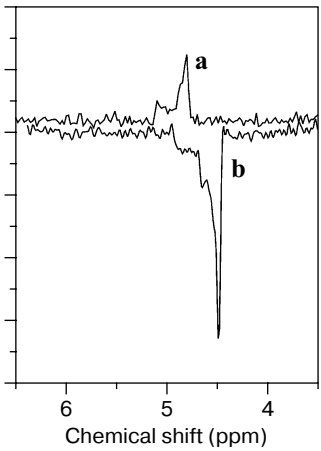

Fig. 8. a Fourier-transformed free induction decay (FT FID) ^{1}H signal from a 6.4 mM TEMPOL in water without MW irradiation. **b** FT FID ^{1}H signal from the same sample irradiated with microwaves (22 mW of incident power). The 0.35 ppm shift is due to heating of the sample by microwaves.

DNP enhancements. In this case, the 24 dB beam splitter was used to reach the maximal MW power at the sample and to keep the detector in linear operation. This dependence reveals that the available maximum MW power of 45 mW cannot saturate one of the hyperfine lines of TEMPOL completely (Fig. 7). The product of relaxation times $T_1T_2 = 3.5 \cdot 10^{-15}$ s^2 estimated from the best fit of the saturation curve [24] correlates well with the W-band results of J. Freed's group [25]. The ^{1}H NMR spectrum of a 6.4 mM aqueous TEMPOL solution is shown in Fig. 8 and demonstrates first DNP enhancements of our spectrometer. The observed DNP enhancement is about -4. The negative sign of the enhancement is due to the characteristics of dipolar coupling inducing the DNP enhancement [10]. More detailed discussion of the DNP results is presented in ref. 26.

5 Conclusions

A 9.4 T DNP spectrometer with a double-resonance structure was developed to study biomolecules in liquid solution. The feasibility of DNP at high fields in liquids was demonstrated with an aqueous TEMPOL solution.

The helix double-resonance structure is of utmost importance for high-field DNP experiments on aqueous solutions to avoid excessive sample heating. Our prototype structure, a cylindrical MW resonator, has severe limitations with respect to the sample volume. Further resonance structures with the larger sample volumes are under development in our laboratory.

In contrast to predictions, DNP enhancement is still significant at magnetic fields as high as 9.2 T. Multiple spin interactions might be useful to obtain even larger enhancements at high magnetic fields in the liquid state.

Acknowledgments

This work has been funded by European Union BioDNP Project. We are grateful to Frank Engelke (Bruker Elektronik GmbH) for fruitful discussions and help to optimize the probe performance and to Bernhard Thiem for the development of the microwave power supply unit. We thank Y. Grishin (Institute of Chemical Kinetics and Combustion, Novosibirsk) for the help in the construction of the orotron device and R. Mett (Medical College of Wisconsin, Milwaukee) for fruitful discussions on the coupling of the cylindrical cavity.

References

1. Bruker: Almanac 2007, p. 28. Bruker Biospin, Rheinstetten (2007)
2. Hu, K.-N., Bajaj, V., Rosay, M., Griffin, R.: J. Chem. Phys. **126**, 044512 (2007)
3. Ardenkjaer-Larsen, J., Fridlund, B., Gram, A., Hansson, G., Hansson, L., Lerche, M., Servin, R., Thaning, M., Golman, K.: Proc. Natl. Acad. Sci. USA **100**, 10158–10163 (2003)
4. Armstrong, B., Han, S.: J. Chem. Phys. **127**, 104508 (2007)
5. McCarney, E.R., Armstrong, B., Lingwood, M., Han, S.: Proc. Natl. Acad. Sci. USA **104**, 1754–1759 (2007)
6. Singel, D.J., Seidel, H., Kendrick, R.D., Yannoni, C.S.: J. Magn. Reson. **81**, 145–161 (1989).
7. Wind, R.A., Hall, R.A., Jurkiewicz, A., Lock, H., Maciel, G.E.: J. Magn. Reson. **110**, 33–37 (1994)
8. Cho, H., Baugh, J., Ryan, C.A., Cory, D.G., Ramanathan, C.: J. Magn. Reson. **187**, 242–250 (2007)
9. Rønne, C., Thrane, L., Åstrand, P.O., Wallqvist, A., Mikkelsen, K.V., Keiding, S.R.: J. Chem. Phys. **107**, 5319–5331 (1997)
10. Hausser, K.N., Stehlik, D.: Adv. Magn. Res. **3**, 79 (1968)
11. Cardin, J.T., Kolachkovski, S.V., Anderson, J.R., Budil, D.E.: Appl. Magn. Reson. **16**, 273–292 (1999)
12. Weis, V., Bennati, M., Rosay, M., Bryant, J.A., Griffin, R.G.: J. Magn. Reson. **140**, 293–299 (1999)
13. Gruber, K., Forrer, J., Schweiger, A., Gunthard, H.H.: J. Phys. E Sci. Instrum. **7**, 569–576 (1973)
14. Engelke, F.: Concepts Magn. Reson. **15**, 129–155 (2002)
15. Nicholson, I., Lurie, D.J., Robb, F.J.L.: J. Magn. Reson. B **104**, 250–255 (1994)
16. Brasch, R.C., London, R.A., Wesbey, G.E., Tozer, T.N., Nitecki, D.E., Williams, R.D., Doemeny, J., Tuck, L.D., Lallemand, D.P.: Radiology **147**, 773 (1983)
17. Afzar, V., Brasch, R.C., Nitecki, D.E., Wolff, S.: Invest. Radiol. **19**, 549 (1984)
18. Rosen, G.M., Griffeth, L.K., Brown, M.A., Drayer, B.P.: Radiology **163**, 239 (1987)
19. Eriksson, U.G., Ogan, M.C., Peng, C.T., Brasch, R.C., Tozen, T.N.: Magn. Reson. Med. **5**, 73 (1987)
20. Slane, J.M.K., Lai, C.S., Hyde, J.S.: Magn. Reson. Med. **3**, 699 (1986)
21. Berliner, L.J.: Pure Appl. Chem. **62**, 247 (1990)
22. Lebedev, Ya.S.: Pure Appl. Chem. **62**, 261 (1990)
23. Marsh, D.: Pure Appl. Chem. **62**, 265 (1990)
24. Poole, C.P.: Electron Spin Resonance: A Comprehensive Treatise on Experimental Techniques, pp. 705–717. Wiley, New York (1967)
25. Hofbauer, W., Earle, K.A., Dunnam, C.R., Moscicki, J.K., Freed, J.H.: Rev. Sci. Instrum. **75**, 1194–1208 (2004)
26. Prandolini, M.F., Denysenkov, V., Gafurov, M., Lyubenova, S., Endeward, B., Bennati, M., Prisner, T.F.: Appl. Magn. Reson. **34**, 399–407 (2008)

Authors' address: Thomas F. Prisner, Institute of Physical and Theoretical Chemistry, J. W. Goethe University, Max-von-Laue-Strasse 7, 60438 Frankfurt am Main, Germany
E-mail: prisner@chemie.uni-frankfurt.de